The ACS Fornax cluster survey. XI. catalog of globular cluster candidates

Jordán, Andrés; Peng, Eric W.; Blakeslee, John P.; Côté, Patrick; Eyheramendy, Susana; Ferrarese, Laura

Publisher's version / Version de l'éditeur:
https://doi.org/10.1088/0067-0049/221/1/13
The Astrophysical Journal Supplement Series, 221, 1, 2015-10-29

The Astrophysical Journal Supplement Series, 221:13 (5pp), 2015 November doi:10.1088/0067-0049/221/1/13

THE ACS FORNAX CLUSTER SURVEY. XI. CATALOG OF GLOBULAR CLUSTER CANDIDATES*

Andrés Jordán[1,2], Eric W. Peng[3,4], John P. Blakeslee[5], Patrick Côté[5], Susana Eyheramendy[2,6], and Laura Ferrarese[5]
[1] Instituto de Astrofísica, Facultad de Física, Pontificia Universidad Católica de Chile, Av. Vicuña Mackenna 4860, 7820436 Macul, Santiago, Chile
[2] Millennium Institute of Astrophysics, Av. Vicuña Mackenna 4860, 7820436 Macul, Santiago, Chile
[3] Department of Astronomy, Peking University, Beijing 100871, China
[4] Kavli Institute for Astronomy and Astrophysics, Peking University, Beijing 100871, China
[5] Herzberg Astronomy and Astrophysics, National Research Council, 5071 West Saanich Road, Victoria, BC V9E 2E7, Canada
[6] Departmento de Estadística, Facultad de Matemáticas, Pontificia Universidad Católica de Chile, Av. Vicuña Mackenna 4860, 7820436 Macul, Santiago, Chile
Received 2015 September 3; accepted 2015 September 28; published 2015 October 29

ABSTRACT

We present catalogs of globular cluster (GC) candidates for 43 galaxies from the ACS Fornax Cluster survey, a program designed to carry out imaging of early-type members of the Fornax cluster using the Advanded Camera for Surveys (ACS) on board the *Hubble Space Telescope*. The procedure to select bona fide GC candidates from the full list of detections is based on model-based clustering methods, similar to those adopted for a survey of 100 galaxies in the Virgo cluster, the ACS Virgo Cluster Survey. For each detected source, we measure its position, magnitudes in the F475W (≈Sloan g) and F850LP (≈Sloan z) bandpasses, half-light radii obtained by fitting point-spread function-convolved King models to the observed light distribution, and an estimate of the probabilty $p_{\rm GC}$ that each cataloged source is a GC. These measurements are presented for 9136 sources, of which 6275 have $p_{\rm GC} \geqslant 0.5$, and are thus likely GCs.

Key words: catalogs – galaxies: elliptical and lenticular, cD – galaxies: star clusters: general

Supporting material: machine-readable table

1. INTRODUCTION

Globular Clusters (GCs) are among the oldest baryonic structures in the universe, which has led to their use as tracers of the assembly of the galaxies to which they are usually bound. Observationally, they are attractive tracers due to their compactness and luminosity: a typical GC has a half-light radius of ≈3 pc and a luminosity of $\approx 10^5 L_\odot$, with well-characterized distributions around these values (e.g., Jordán et al. 2005, 2007b).

The largest repository of GCs in the local universe is the Virgo Cluster at a distance of ≈16.5 Mpc (Mei et al. 2007; Blakeslee et al. 2009), followed by the much more compact and less rich Fornax cluster at ≈20 Mpc (Blakeslee et al. 2009). The ACS Virgo and Fornax Cluster Surveys (Côté et al. 2004; Jordán et al. 2007a) had as one of their major aims the detection and characterization of the GC populations around 100 early-type galaxies in Virgo and 43 in Fornax (these surveys will be referred to as ACSVCS and ACSFCS, respectively, in what follows). Observations were carried out with the Advanced Camera for Surveys (ACS) on board the *Hubble Space Telescope* (*HST*). ACS makes it possible to detect ≳90% of the GC population that fell within the ACS field of view for each of the targeted galaxies in a single *HST* orbit, and to do so in two bands: F475W (≈Sloan g) and F850LP (≈Sloan z). In the case of Virgo, the ACSVCS detected 20,375 spatially resolved sources around their target galaxies, of which 12,763 were considered to be bona fide GC candidates, approximately two orders of magnitude more than the GC population in our Galaxy. Such a massive census of GCs in the local universe in two bands was made possible by the large improvements in sensitivity that ACS delivered over its predecessor, the *Wide Field Planetary Camera 2*, which had already achieved great advances in the study of GC systems around selected galaxies in Virgo.

In this paper, we present a catalog of 9136 spatially resolved sources detected around the target early-type galaxies of the ACSFCS, complementing the catalog of 20,375 sources presented previously for the Virgo sample by Jordán et al. (2009). For each detected source, we present estimates of its position, its magnitudes in the F475W and F850LP bandpasses, and its half-light radii by fitting a point-spread function (PSF)-convolved King model to the observed light distribution. The catalog presented here was used in previous papers studying various properies of the GC systems of the ACSFCS target galaxies, namely, their half-light radii (Masters et al. 2010), luminosity functions (Villegas et al. 2010), color–magnitude relations (Mieske et al. 2010), and color gradients (Liu et al. 2011).

2. GC CATALOGS

The detection, selection, and characterization of the sources presented in this paper has been throughly documented in previous publications. The data reduction procedures and rough initial culling of ACSFCS sources are detailed in Jordán et al. (2007a). These procedures were in turn devised to be homogeneous with respect to those adopted in ACSVCS and are described in Jordán et al. (2004). All of the sources that satisfy the rough initial culling belong mainly to three populations: foreground (Milky Way) stars, background galaxies, and GCs.

For completeness, here we briefly describe our adopted procedure to select bona fide GC candidates from those sources that satisfy the initial selection criteria; a full, detailed account

* Based on observations with the NASA/ESA *Hubble Space Telescope* obtained at the Space Telescope Science Institute, which is operated by the Association of Universities for Research in Astronomy, Inc., under NASA contract NAS 5-26555.

is given in Jordán et al. (2009). We begin by describing the measurements upon which the selection is based.

1. Magnitudes in the F475W and F850LP bandpasses, denoted in what follows by g_{475} and z_{850}, respectively. We measured aperture magnitudes and model magnitudes obtained by fitting King (1966) models convolved with the PSF. Aperture magnitudes were measured with SExtractor (Bertin & Arnouts 1996) as described in Jordán et al. (2004), with aperture corrections applied as described in Section 3 of Jordán et al. (2009). Model magnitudes were obtained using the procedure described in the Appendix of Jordán et al. (2005), with aperture corrections applied as described in Section 3 of Jordán et al. (2009).
2. Half-light radii measured as described in Jordán et al. (2005, 2007a). We estimated half-light radii in the g_{475} and z_{850} bands, denoted by $r_{h,g_{475}}$ and r_h, z_{850}, respectively, and defined the half-light radius of each souce r_h to be the straight average of the g_{475}- and z_{850}-band measurements, i.e., $r_h \equiv 0.5(r_{h,z_{850}} + r_{h,g_{475}})$.

The first step was to eliminate all of the sources that were consistent with being point sources by imposing the condition $r_h > 0''.0096$, or $\approx$0.2 ACS pixels. All of the sources that meet this condition are cataloged in this paper.[7]

Having eliminated the unresolved sources, we were left with the task of separating GCs from background clusters. For that purpose, we modeled the observed distribution of sources in the $z_{850}-r_h$ plane as a mixture model with two components. The GC component, $d_{\rm GC}$, is assumed to be distributed as

$$d_{\rm GC}(z_{850}, r_h \mid \mu_{rh}) = \frac{1}{\sqrt{2\pi}\,\sigma} \exp\left[-\frac{(z_{850} - 22.8)^2}{2\sigma^2}\right] \times g_{\rm gc}(r_h \mid \mu_{rh}), \quad (1)$$

where $\sigma = 1.3$ mag[8] and $g_{\rm gc}$ is an empirically determined distribution for r_h. The value of 22.8 for the mean GC z_{850} magnitude was chosen to be 0.1 magnitudes fainter than the one we used for Virgo based on the mean difference of the GC luminosity function means for the Virgo and Fornax galaxies reported in Ferrarese et al. (2000).[9] The only free parameter of $d_{\rm GC}$ is the mean half-light radius μ_{rh}; the rationale for assuming this distribution is detailed in Section 2.1.1 of Jordán et al. (2009). The background galaxy component is a fixed distribution $d_{\rm cont}(z_{850}, r_h)$ which was constructed using control fields as described in Jordán et al. (2009). The full model of the joint ditribution of sources for a given galaxy in the ACSFCS

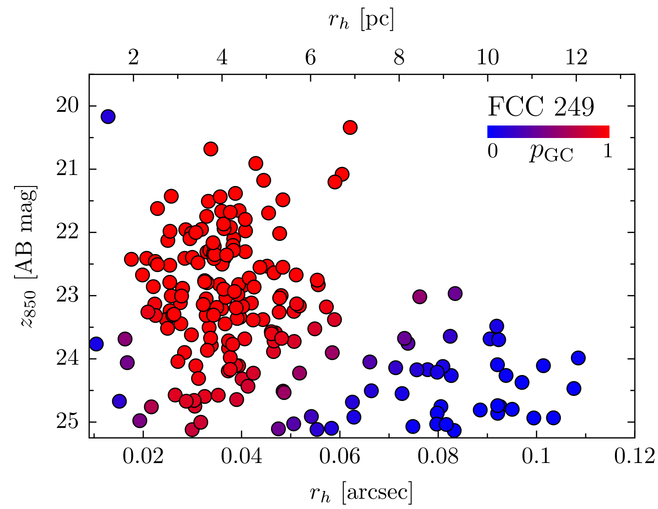

Figure 1. Resolved sources around the early-type galaxy FCC 249 (NGC 1419) plotted in the r_h–z_{850} plane. Points are color coded based on their estimated probabilty of being a globular cluster $p_{\rm GC}$ according to the color bar shown in the figure.

sample is then given by

$$M(z_{850}, r_h \mid \mu_{rh}, f_{\rm GC}) = \left[f_{\rm GC}\, d_{\rm GC}(z_{850}, r_h \mid \mu_{rh}) + (1 - f_{\rm GC}) d_{\rm cont}(z_{850}, r_h)\right]. \quad (2)$$

Here, $f_{\rm GC}$ and $1-f_{\rm GC}$ are the fractions of the sample that are expected to be GCs and background galaxies (contaminants), respectively. We estimate the two parameters $\{\mu_{rh}, f_{\rm GC}\}$ in our model using the Expectation–Maximization algorithm as detailed in Jordán et al. (2009). Once the parameters have been estimated, for each source we can calculate the probability $p_{\rm GC}$ of being a GC via the assignment

$$p_{\rm GC} = \frac{f_{\rm GC}\, d_{\rm GC}(z_{850}, r_h \mid \mu_{\rm rh})}{f_{\rm GC}\, d_{\rm GC}(z_{850}, r_h \mid \mu_{rh}) + (1 - f_{\rm GC}) d_{\rm cont}(z_{850}, r_h)}, \quad (3)$$

and, given that there are just two components, the corresponding probability $p_{\rm cont}$ of it being a contaminant is given simply by $p_{\rm cont} = 1 - p_{\rm GC}$. In a final step, $p_{\rm GC} \equiv 1$ is assigned to all of the sources satisfying $z < 23$ mag and 1.5 pc $< r_h <$ 4 pc, as we want to consider these sources as bona fide GC candidates regardless of the exact value of $p_{\rm GC}$ returned by the algorithm. Due to the high level of contamination of faint extended objects, we also set $p_{\rm GC} = 0$ for $z_{850} > 25.25$ mag and $r_h > 10$ pc. For illustration purposes, Figure 1 shows the resolved sources around the E0 galaxy FCC 249 in the r_h–z_{850} plane, with points color coded according to the values of $p_{\rm GC}$ assigned by the algorithm.

Table 1 presents for each ACSFCS galaxy the parameter estimates of the mixture model described by Equation (2). In Table 2, we present our full catalog of resolved sources for all of the galaxies in ACSFCS[10]; a Hess diagram in the

[7] In Jordán et al. (2009), it is stated that the cataloged sources for ACSVCS are all those which satisfy the rough initial culling detailed in Jordán et al. (2004), but this is incomplete as an additional cut in r_h, similar to the one described here, was also applied before cataloging.

[8] In Jordán et al. (2006, 2007b) we found that the dispersion of the GC luminosity function when modeled by a Gaussian depends systematically on the galaxy luminosity, with $\sigma \approx 1.4$ for giant early-types and decreasing to $\sigma \approx 0.8$ for the faintest members in the ACSVCS sample. We kept a single value of $\sigma = 1.3$ in this work to maintain homogeneity with the selection procedure adopted in ACSVCS. Additionally, we want to include in our selection procedures the faint galaxies which have small numbers of GCs.

[9] Based on the ACSFCS data we present in this work, we later updated this value to 0.2 ± 0.04 (Villegas et al. 2010).

[10] We note that for FCC 213 (NGC 1399) the catalog presented here corresponds only to objects present in the imaging acquired as part of the ACSFCS, but there is a set of ACS observations in the F606W filter that allows estimation of sizes for GCs at larger galactocentric radii than those cataloged in this work (Puzia et al. 2014).

Table 1
Maximum-likelihood Parameters of Mixture Model

ID (1)	μ_{r_h} (pc) (2)	$f_{\rm GC}$ (3)	ID (1)	μ_{r_h} (pc) (2)	$f_{\rm GC}$ (3)
FCC21	3.53	0.602	FCC255	3.57	0.606
FCC213	2.94	0.938	FCC277	3.64	0.473
FCC219	2.94	0.867	FCC55	3.87	0.381
NGC1340	2.97	0.684	FCC152	4.06	0.282
FCC167	3.23	0.743	FCC301	3.72	0.288
FCC276	2.72	0.856	FCC335	4.30	0.232
FCC147	2.95	0.855	FCC143	3.39	0.564
IC2006	3.43	0.715	FCC95	4.01	0.331
FCC83	3.23	0.766	FCC136	3.92	0.336
FCC184	3.00	0.787	FCC182	3.81	0.452
FCC63	3.36	0.804	FCC204	4.27	0.274
FCC193	4.01	0.450	FCC119	4.20	0.209
FCC170	3.13	0.588	FCC90	4.02	0.315
FCC153	3.69	0.590	FCC26	4.12	0.296
FCC177	3.82	0.527	FCC106	3.94	0.283
FCC47	3.34	0.765	FCC19	3.82	0.243
FCC43	3.96	0.326	FCC202	3.31	0.730
FCC190	4.01	0.668	FCC324	4.28	0.324
FCC310	3.20	0.424	FCC288	3.76	0.236
FCC249	3.70	0.757	FCC303	3.85	0.341
FCC148	3.26	0.527	FCC203	4.00	0.383
FCC100	4.17	0.420	…	…	…

Note. Key to columns—(1) Galaxy ID; (2) mean half-light radius of GC component (assuming $D = 20$ Mpc); (3) estimated fraction of the total sample of the GC component. The corresponding quantity for the contaminants component, $f_{\rm cont}$ is given by $f_{\rm cont} \equiv 1 - f_{\rm GC}$.

r_h–z_{850} plane for all of the cataloged sources is shown in Figure 2. The first column in Table 2 is the galaxy identifier, primarily taken from the Fornax Cluster Catalog (FCC; Ferguson 1989), except for IC 2006 and NGC 1380, which were not in the footprint of the FCC. Columns (2) and (3) give the R.A. α (J2000) and decl. δ (J2000) of each source, and column (4) gives the projected distance to the center of the host galaxy in arcseconds. Columns (5) and (6) give the total King model magnitude and the total magnitude inferred from a $0\farcs2$ aperture for the z_{850} band. These magnitudes have been dereddened, as described in Section 5.1 in Jordán et al. (2007a), and have had aperture corrections applied as described in Section 3 of Jordán et al. (2009). Columns (7) and (8) give the corresponding quantities for the g_{475} band. Columns (9) and (10) give the best-fit half-light radii of the PSF-convolved King (1966) models in arcseconds for the z_{850} and g_{475} bands, respectively. The uncertainties do not include systematic uncertainties arising from the PSF modeling, which can be estimated to be of the order of $\approx 0\farcs005$ (see Jordán et al. 2005). In order to convert the half-light radii to physical units, we can use the SBF distances to our galaxies presented in Blakeslee et al. (2009). Column (11) gives the value of $p_{\rm GC}$ for each source. Column (12) gives the adopted value of $E(B - V)$ taken from the DIRBE maps of Schlegel et al. (1998). Finally, columns (13) and (14) give the galaxy plus "sky" background in counts s^{-1} present under each source in the g_{475} and z_{850} bands, respectively. These quantities are necessary to estimate the expected survey completeness at the position of each source using the data presented in Tables 2 and 3 of Jordán et al. (2009), which are also applicable to the ACSFCS.

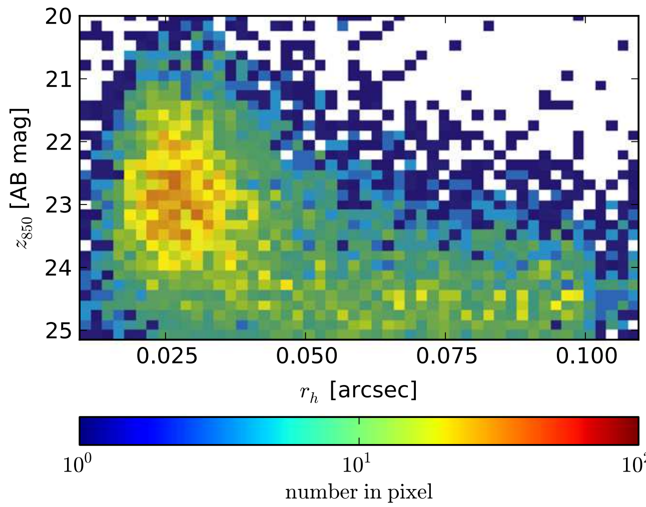

Figure 2. Hess diagram in the r_h–z_{850} plane for all sources cataloged in this work.

3. SUMMARY

We have presented the results of our photometric and structural parameter measurements for 9136 spatially resolved sources which satisfy the rough selection procedures described Jordán et al. (2007a). For each cataloged source, we measure its position, g_{475} and z_{850} magnitudes, and half-light radii. We estimate the probability for each source to be a GC using a model-based mixture model and find that 6275 sources are likely to be GCs lying within the ACS field of view around our target galaxies.

Previously, we presented a similar catalog for 100 galaxies in the Virgo cluster (Jordán et al. 2009). In combination, the ACSVCS and ACSFCS catalogs present measurements of the magnitudes, positions, and half-light radii for over 19,000 likely GCs in the two most prominent galaxy clusters in the local universe ($D \lesssim 25$ Mpc). The catalogs are constructed in a very homogeneous fashion and can be directly joined as a single catalog of resolved sources around 143 Virgo and Fornax galaxies. In terms of the numbers of likely GCs cataloged, new wide-field, ground-based surveys of nearby structures such as the Next Generation Virgo Survey (Ferrarese et al. 2012; Durrell et al. 2014) will soon provide larger yields and better photometric characterization, but the combined ACSFCS and ACSFCS GC catalogs remain unique in providing size estimates thanks to the resolving power of *HST*. As such, it should provide a very useful compliment to spectroscopic studies of GCs with the next generation ground-based telescopes, whose light-gathering power should allow the measurement of internal velocity dispersions for interesting numbers of sources and for which the half-light radii presented here will be very useful to be able to provide mass estimates.

Support for program GO-10217 was provided through a grant from the Space Telescope Science Institute, which is operated by the Association of Universities for Research in Astronomy, Inc, under NASA contract NAS5-26555. A.J. and S.E. acknowledge support from the Ministry of Economy, Development, and Tourism's Millennium Science Initiative

Table 2
Photometric and Structural Catalog of Sources[a,b]

ID (1)	α (J2000) (2)	δ (J2000) (3)	$d_{\rm gal}$ ($''$) (4)	m_z (5)	$m_{z,\rm ap}$ (6)	m_g (7)	$m_{g,\rm ap}$ (8)	$r_{h,z}$ (9)	$r_{h,g}$ (10)	$p_{\rm GC}$ (11)	$E(B-V)$ (12)	b_z (13)	b_g (14)
21	50.6728957	−37.2095599	5.075	22.144 ± 0.204	22.332 ± 0.091	23.922 ± 0.152	23.917 ± 0.097	0.0774 ± 0.0241	0.0671 ± 0.0152	0.81	0.021	10.1850	7.9620
21	50.6745804	−37.2101309	6.549	23.284 ± 0.134	23.230 ± 0.132	24.958 ± 0.299	24.919 ± 0.113	0.0271 ± 0.0063	0.0254 ± 0.0095	0.97	0.021	4.5010	3.5840
21	50.6722922	−37.2105599	9.040	21.575 ± 0.034	21.532 ± 0.031	22.681 ± 0.021	22.649 ± 0.019	0.0334 ± 0.0035	0.0365 ± 0.0016	1.00	0.021	4.7960	3.8120
21	50.6745959	−37.2109056	9.265	20.737 ± 0.028	20.705 ± 0.024	21.793 ± 0.038	21.773 ± 0.034	0.0193 ± 0.0042	0.0218 ± 0.0038	1.00	0.021	3.0480	2.4190
21	50.6718051	−37.2105049	9.663	20.913 ± 0.090	20.883 ± 0.033	21.985 ± 0.034	21.988 ± 0.032	0.0329 ± 0.0065	0.0383 ± 0.0045	1.00	0.021	4.7660	3.7840
21	50.6712169	−37.2100478	9.710	22.130 ± 0.079	22.111 ± 0.063	23.728 ± 0.126	23.689 ± 0.054	0.0491 ± 0.0073	0.0237 ± 0.0063	1.00	0.021	5.1170	4.1070
21	50.6751601	−37.2054202	11.314	18.697 ± 0.009	18.639 ± 0.009	20.058 ± 0.017	20.028 ± 0.011	0.0126 ± 0.0021	0.0123 ± 0.0014	0.01	0.021	3.3880	2.6960
21	50.6768338	−37.2061849	11.608	20.976 ± 0.025	20.940 ± 0.018	22.845 ± 0.027	22.803 ± 0.026	0.0333 ± 0.0023	0.0272 ± 0.0021	1.00	0.021	3.8160	3.1540
21	50.6779378	−37.2076265	11.925	22.727 ± 0.382	22.681 ± 0.062	24.016 ± 1.524	23.978 ± 0.053	0.0205 ± 0.0070	0.0299 ± 0.0062	1.00	0.021	3.1970	2.5620
21	50.6782065	−37.2086042	12.383	21.715 ± 0.031	21.675 ± 0.034	23.058 ± 0.035	23.031 ± 0.036	0.0142 ± 0.0029	0.0158 ± 0.0029	0.38	0.021	2.6340	2.1580
21	50.6697109	−37.2097413	12.923	22.549 ± 0.246	22.486 ± 0.062	23.195 ± 0.047	23.176 ± 0.042	0.0186 ± 0.0063	0.0251 ± 0.0034	1.00	0.021	3.5530	2.9190
21	50.6759959	−37.2050817	13.363	23.521 ± 0.167	23.520 ± 0.131	24.861 ± 0.682	25.119 ± 0.255	0.0641 ± 0.0145	0.0818 ± 0.1709	0.27	0.021	2.9890	2.4380
21	50.6740764	−37.2121389	13.491	20.383 ± 0.936	20.409 ± 0.040	21.657 ± 0.260	21.642 ± 0.045	0.0068 ± 0.0046	0.0130 ± 0.0042	0.03	0.021	2.0680	1.6280
21	50.6692610	−37.2093767	13.739	19.078 ± 0.017	19.126 ± 0.007	20.374 ± 0.023	20.420 ± 0.010	0.0472 ± 0.0016	0.0476 ± 0.0007	0.83	0.021	3.1500	2.5470
21	50.6707108	−37.2054256	14.056	22.765 ± 0.195	22.735 ± 0.057	24.041 ± 0.062	24.005 ± 0.057	0.0308 ± 0.0121	0.0369 ± 0.0087	1.00	0.021	1.9190	1.6080
21	50.6768231	−37.2115322	14.087	17.353 ± 0.020	17.335 ± 0.014	18.581 ± 0.011	18.572 ± 0.011	0.0266 ± 0.0022	0.0291 ± 0.0018	1.00	0.021	1.6800	1.2960
21	50.6688347	−37.2083051	14.501	22.060 ± 0.066	22.109 ± 0.032	23.174 ± 0.145	23.411 ± 0.041	0.0746 ± 0.0052	0.0812 ± 0.0197	0.69	0.021	2.5300	2.1020
21	50.6786708	−37.2099702	14.824	22.394 ± 0.353	22.332 ± 0.029	23.573 ± 0.031	23.533 ± 0.031	0.0114 ± 0.0050	0.0179 ± 0.0046	0.46	0.021	1.8010	1.4670
21	50.6785854	−37.2105139	15.464	22.436 ± 0.039	22.377 ± 0.012	23.722 ± 0.523	23.706 ± 0.101	0.0163 ± 0.0023	0.0230 ± 0.0126	1.00	0.021	1.6050	1.2640

Notes. Key to columns—(1) Galaxy identifier; (2)–(3) J2000 R.A. (α) and decl. (δ) in decimal degrees; (4) Galactocentric distance in arcseconds; (5) z_{850}-band model magnitude obtained from the best-fit PSF-convolved King model and an aperture correction as per Equation (9) in Jordán et al. (2009); (6) z_{850}-band average correction aperture magnitude inferred from a $0\farcs2$ aperture and an aperture correction as per Equation (10) in Jordán et al. (2009); (7) same as (5) but for the g_{475} band; (8) same as (6) but for the g_{475} band; (9)–(10) best-fit half-light radii measured in the z_{850} and g_{475} bands, respectively; (11) probability that the source is a GC according to the maximum-likelihood estimate of our asumed mixture model (see Section 2 in this work and in Jordán et al. 2009); (12) foreground $E(B-V)$ assumed for this source. The corrections for foreground reddening were taken to be $A_g = 3.634E(B-V)$ and $A_z = 1.485E(B-V)$ in the g and z bands, respectively (see Jordán et al. 2004); (13) background in the z_{850} band (counts s^{-1}); (14) background in the g_{475} band (counts s^{-1}).
[a] Table 2 is presented in its entirety as supplemental material. A portion is shown here for guidance regarding its form and content.
[b] Table 2 present the structural and photometrical catalog of all ACSFCS sources that satisfy the selection criteria presented in Section 2.6 in Jordán et al. (2004), modified as described in Section 5.1 of Jordán et al. (2007a), and that have $r_h > 0\farcs0096$. To select a sample of bona fide GCs the sources should be restricted to those having $p_{\rm GC} \geqslant 0.5$.

(This table is available in its entirety in machine-readable form.)

through grant IC120009, awarded to The Millennium Institute of Astrophysics, MAS. A.J. acknowledges additional support from BASAL CATA PFB-06.

REFERENCES

Bertin, E., & Arnouts, S. 1996, A&AS, 117, 393
Blakeslee, J. P., Jordán, A., Mei, S., et al. 2009, ApJ, 694, 556
Côté, P., Blakeslee, J. P., Ferrarese, L., et al. 2004, ApJS, 153, 223
Durrell, P. R., Côté, P., Peng, E. W., et al. 2014, ApJ, 794, 103
Ferguson, H. C. 1989, AJ, 98, 367
Ferrarese, L., Côté, P., Cuillandre, J.-C., et al. 2012, ApJS, 200, 4
Ferrarese, L., Ford, H. C., Huchra, J., et al. 2000, ApJS, 128, 431
Jordán, A., Blakeslee, J. P., Côté, P., et al. 2007a, ApJS, 169, 213
Jordán, A., Blakeslee, J. P., Peng, E. W., et al. 2004, ApJS, 154, 509
Jordán, A., Côté, P., Blakeslee, J. P., et al. 2005, ApJ, 634, 1002
Jordán, A., McLaughlin, D. E., Côté, P., et al. 2006, ApJL, 651, L25
Jordán, A., McLaughlin, D. E., Côté, P., et al. 2007b, ApJS, 171, 101
Jordán, A., Peng, E. W., Blakeslee, J. P., et al. 2009, ApJS, 180, 54
King, I. R. 1966, AJ, 71, 64
Liu, C., Peng, E. W., Jordán, A., et al. 2011, ApJ, 728, 116
Masters, K. L., Jordán, A., Côté, P., et al. 2010, ApJ, 715, 1419
Mei, S., Blakeslee, J. P., Côté, P., et al. 2007, ApJ, 655, 144
Mieske, S., Jordán, A., Côté, P., et al. 2010, ApJ, 710, 1672
Puzia, T. H., Paolillo, M., Goudfrooij, P., et al. 2014, ApJ, 786, 78
Schlegel, D. J., Finkbeiner, D. P., & Davis, M. 1998, ApJ, 500, 525
Villegas, D., Jordán, A., Peng, E. W., et al. 2010, ApJ, 717, 603